Title
Dissipative response to excess light is catalyzed in monomeric and trimeric light harvesting complexes by two independent mechanisms

Authors
Dall'Ostoa, L
Cazzanigaa, S
Bressana, M
et al.

Publication Date
2016

Peer reviewed

nature plants

ARTICLES

PUBLISHED: 10 APRIL 2017 | VOLUME: 3 | ARTICLE NUMBER: 17033

Two mechanisms for dissipation of excess light in monomeric and trimeric light-harvesting complexes

Luca Dall'Osto[1†], Stefano Cazzaniga[1†], Mauro Bressan[1], David Paleček[2], Karel Žídek[2], Krishna K. Niyogi[3,4], Graham R. Fleming[4,5,6], Donatas Zigmantas[2] and Roberto Bassi[1,7*]

Oxygenic photoautotrophs require mechanisms for rapidly matching the level of chlorophyll excited states from light harvesting with the rate of electron transport from water to carbon dioxide. These photoprotective reactions prevent formation of reactive excited states and photoinhibition. The fastest response to excess illumination is the so-called non-photochemical quenching which, in higher plants, requires the luminal pH sensor PsbS and other yet unidentified components of the photosystem II antenna. Both trimeric light-harvesting complex II (LHCII) and monomeric LHC proteins have been indicated as site(s) of the heat-dissipative reactions. Different mechanisms have been proposed: energy transfer to a lutein quencher in trimers, formation of a zeaxanthin radical cation in monomers. Here, we report on the construction of a mutant lacking all monomeric LHC proteins but retaining LHCII trimers. Its non-photochemical quenching induction rate was substantially slower with respect to the wild type. A carotenoid radical cation signal was detected in the wild type, although it was lost in the mutant. We conclude that non-photochemical quenching is catalysed by two independent mechanisms, with the fastest activated response catalysed within monomeric LHC proteins depending on both zeaxanthin and lutein and on the formation of a radical cation. Trimeric LHCII was responsible for the slowly activated quenching component whereas inclusion in supercomplexes was not required. This latter activity does not depend on lutein nor on charge transfer events, whereas zeaxanthin was essential.

Plants and algae use light as an energy source for carbon dioxide (CO_2) fixation into sugars. Their photosystems are composed of a core complex, where charge separation events fuel electron transport from H_2O to $NADP^+$, and an antenna system, which expands the absorption cross-section. Large antennas favour energy supply in low-light conditions, yet at high-light (HL) intensities they cause excess excitation beyond the maximal capacity for photochemical reactions. Unquenched singlet excited states of chlorophyll (^{1}Chl*) undergo intersystem crossing and the resulting triplets (^{3}Chl*) react with oxygen (O_2) to yield singlet oxygen ($^1O_2$) and photoinhibition. Within the photosynthetic machinery, photosystem II (PSII) and its reaction centre (RC), the special Chl pair P680, have been indicated as the primary target of photoinhibition[1]. Avoiding photoinhibition in the ever-changing environment has likely shaped mechanisms that regulate PSII quantum efficiency[2]. This set of inducible mechanisms, collectively referred to as NPQ (non-photochemical quenching), facilitate heat dissipation of the ^{1}Chl* state energy and can thus be monitored as a light-dependent decrease of Chl fluorescence. Under full sunlight, NPQ converts as much as 80% of absorbed photons into heat, thereby reducing the quantum yield of PSII (reviewed in[3]).

NPQ can be dissected into a number of kinetic components: qE, qZ, qM and qI[4–6]. qE (energy quenching) is the dominant NPQ component, which is rapidly induced (within 20–60 s), is reversible in seconds and is triggered by the over-acidification of the thylakoid membrane. Signal transduction of luminal acidification involves PsbS, through protonation of two lumen-exposed glutamate residues[7]. Since PsbS is an atypical LHC protein, not binding pigments[8,9], quenching reactions must be located in interacting pigment-binding subunits of PSII, located in grana partitions together with PsbS.

PSII is made by a Chl *a*- and β-carotene-binding dimeric core complex[10] surrounded by an antenna system binding Chl *a*, *b* and xanthophylls. Antennas are arranged into an inner layer of mononomeric LHC proteins called CP29, CP26 and CP24 (encoded by the *Lhcb4*, *Lhcb5* and *Lhcb6* genes, respectively) and an outer layer of trimeric LHCII subunits made of *Lhcb1-Lhcb3* gene products[11]. Together, the PSII core and antenna system form supercomplexes[12], whose composition undergoes dynamic changes depending on acclimation to light conditions[13] and NPQ activation[14]. Several lines of evidence suggest that the site of quenching is located within the PSII antenna system: (1) lutein (Lut) and zeaxanthin (Zea), ligands of LHC proteins, are essential for NPQ activity[15]; (2) Chl *b*-less plants lack both LHCs and qE[16] although depletion of PSII core complexes does not affect qE activity[17]; (3) DCCD binding to lumen-exposed protonatable residues of LHCs inhibits qE[18]; (4) quenching induced by aggregation in isolated LHC proteins shares spectroscopic features with qE[19]. Nevertheless, identification of PsbS partners in quenching reactions is complex due to the high number of gene products involved: in *Arabidopsis*, only Lhcb5 and Lhcb6 subunits are encoded by single genes, whereas Lhcb4 and LHCII are encoded, respectively, by three and nine genes[11].

[1]Dipartimento di Biotecnologie, Università di Verona, Strada Le Grazie 15, 37134 Verona, Italy. [2]Department of Chemical Physics, Lund University, Getingevägen 60, Lund S-22241, Sweden. [3]Howard Hughes Medical Institute, Department of Plant and Microbial Biology, University of California, Berkeley 94720-3102, California, USA. [4]Molecular Biophysics and Integrated Bioimaging Division, Lawrence Berkeley National Laboratory, Berkeley 94720, California, USA. [5]Graduate Group in Applied Science and Technology, University of California, Berkeley 94720, California, USA. [6]Department of Chemistry, Hildebrand B77, University of California, Berkeley 94720-1460, California, USA. [7]Consiglio Nazionale delle Ricerche (CNR), Istituto per la Protezione delle Piante (IPP), Via Madonna del Piano 10, 50019 Sesto Fiorentino, Firenze, Italy. †These authors contributed equally to the work. *e-mail: roberto.bassi@univr.it

Also, open questions include the role of Zea, which enhances the amplitude of quenching reactions[20], and the biophysical mechanism(s) by which the quenching reactions are initiated. Proposals include (1) Chl-Chl interactions, yielding into a mixing of charge transfer (CT) states and excitonic states, acting as quenchers[21,22]; (2) formation of short-living Chl-xanthophyll excited states, which serve as traps for $^1Chl^*$[19,23]; (3) CT events in a Chl *a*–Zea heterodimer, followed by charge recombination to the ground state[24,25]. Interaction between Chl *a* and Zea might be promoted by a conformational change from the interaction of protonated PsbS with CP29[26] or between PsbS and LHCII, forming a Zea–PsbS/LHCII complex at the interface[27]. It was also shown that $^1Chl^*$ quenching can occur by the formation of a transient Chl^--Lut^+ state[28]. The large number of models for the NPQ mechanism clearly shows that knowledge is limited: many hypotheses are based on measurements *in vitro*, which, although mimicking, might not closely reflect *in vivo* phenomena.

In this work, we isolated and characterized the *Arabidopsis koLhcb4.1 koLhcb4.2 koLhcb5* triple mutant (hereafter referred to as *NoM*), which lacks all monomeric Lhcbs but retains a full trimeric LHCII complement. Further, we introduced the *npq1, lut2* and *npq4* mutations, preventing, respectively, Zea and Lut synthesis or PsbS accumulation. Lack of monomeric antenna complexes delayed substantially the onset of quenching reactions and changed the xanthophyll-dependence of the residual NPQ activity, implying the fast- and slow-activated components contributing to NPQ in wild type were catalysed, respectively, by monomeric and trimeric components of the PSII antenna system.

Results

NoM is a triple knock-out mutant of *Arabidopsis*, lacking all monomeric Lhcb subunits of the PSII. *NoM* plants were obtained by crossing homozygous transfer DNA (T-DNA) mutants carrying insertions in genes encoding *Lhcb4.1*, *Lhcb4.2* and *Lhcb5*, as previously described[29–31]. When grown in a climate chamber for 4 weeks under controlled conditions (150 µmol photons m^{-2} s^{-1}, 23 °C, 8/16 day/night), *NoM* plants showed a significant growth reduction with respect to wild-type plants (Fig. 1 and Table 1). The possibility that such a phenotype was due to the presence of unrelated mutation(s) was ruled out since parental knock-out (KO) mutants were not affected in their growth[29–31]. Moreover, the reduced growth was not due to altered development, since leaf formation rates were similar in the two genotypes (Supplementary Fig. 1a).

Dark-adapted *NoM* plants showed a high Chl fluorescence phenotype: images of minimum Chl fluorescence (F_0) were captured and false-colour images relative to F_0 parameter were generated from the fluorescence data. A far higher emission in the mutant suggested that absorbed light energy was not used for photochemistry as efficiently as in the wild type, thus yielding an enhanced excitation level in the antenna (Fig. 1).

The quantum efficiency of PSII photochemistry was assessed by Chl fluorescence analysis *in vivo*[32]. The ratio of variable to maximum fluorescence (F_v/F_m), that is the maximal photochemical yield of the PSII RC, was 0.57 ± 0.02 in *NoM* versus 0.81 ± 0.01 in wild type (Table 1), indicating partial loss of PSII activity. *NoM* leaves, illuminated at 150 µmol photons m^{-2} s^{-1} for 25 min, showed a significant reduction in both maximal efficiency of PSII photochemistry (F'_v/F'_m) and the efficiency of PSII-harvested light for Q_A reduction (Φ_{PSII}), with respect to wild type. These effects suggest a defective connection of the LHC antenna to the PSII RC, consistent with the increased F_0 level compared to wild type (Table 1 and Fig. 1).

NoM plants grown in control light showed a slight but significant decrease in Chl content per leaf area compared to wild type as well as lower Chl *a*/*b* and Chl/Car ratios (Table 1). In dark-adapted plants, the content of xanthophylls (neoxanthin, Vio and Lut) was higher in *NoM*, whereas the level of β-carotene was unaffected. Synthesis of Zea, induced by exposing plants for 20 min to HL (1,200 µmol photons m^{-2} s^{-1}, 23 °C), was the same in both genotypes (Supplementary Table 1).

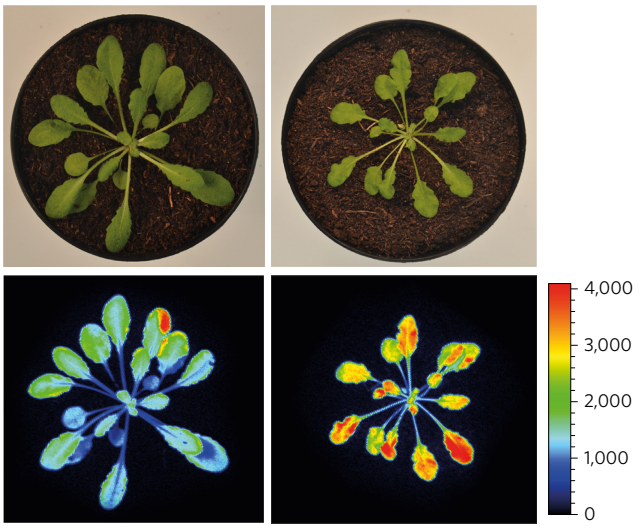

Figure 1 | Phenotype of wild-type and *NoM* plants. Upper panels: plants were grown for 6 weeks at 150 µmol photons m^{-2} s^{-1}, 23 °C, 8/16 h light/dark. Lower panels: imaging of minimal Chl fluorescence (F_0) of wild-type and *NoM* plants. Relative fluorescence is indicated by the colour scale bar (arbitary units).

The SDS–polyacrylamide gel electrophoresis (SDS–PAGE) of thylakoid membrane polypeptides showed that *NoM* plants completely lacked Lhcb4 (Fig. 2a), despite still containing the *Lhcb4.3* gene, in agreement with previous reports that Lhcb4.3 did not accumulate in mutants deleted in both Lhcb4.1 and Lhcb4.2[30]. The band corresponding to Lhcb6 was also missing, because of destabilization in the absence of its docking site CP29[30]. The *NoM* mutant is, thus, lacking all monomeric LHC proteins of PSII.

The organization of pigment-binding complexes was then analysed by non-denaturing PAGE (Fig. 2b). The photosystem I (PSI) formed a single green band at 650 kDa including the core complex and its antenna moiety. In the case of PSII instead, the component pigment–proteins migrated as multiple bands: namely, the monomeric Lhcbs, the trimeric LHCII, the Lhcb4–Lhcb6–LHCII-M complex and the PSII core. The upper region of the gel contained undissociated supercomplexes, which formed multiple green bands according to their different LHC complements. The pattern from *NoM* thylakoids differed in the lack of all PSII supercomplex bands, as well as of the Lhcb4–Lhcb6–LHCII-M complex. The mobility and abundance of PSI-LHCI, PSII core and monomeric Lhcbs were unaffected, whereas the abundance of the trimeric LHCII was enhanced in *NoM* with respect to wild type.

Quantification of pigment-binding proteins by immunotitration (Fig. 2c,d) yielded the same PSI/PSII (PsaA/CP47) ratio for wild type and *NoM* and an increased LHCII/PSII ratio, suggesting the mutant reacted to the lack of monomeric LHCs by over-accumulating (+60%) the trimeric LHCII antenna.

NPQ of chlorophyll fluorescence. We assessed the ability of wild type and *NoM* to undergo quenching of Chl fluorescence upon exposure to HL and analysed the known components of the NPQ mechanism including the abundance of the luminal pH sensor PsbS, the extent of thylakoid lumen acidification and the capacity for Zea synthesis. PsbS was present in both genotypes and its abundance with respect to LHCII was similar in *NoM* versus wild type (Supplementary Fig. 2a). Measuring lumen acidification

Table 1 | Measurement of Chl and Car content, fresh weight and key photosynthetic parameters on leaves of *Arabidopsis* wild type and *NoM*.

	Chl a/b	Chl/Car	µg Chl per cm^2	Fresh weight (g)	F_o/Chl (a.u.)	F_v/F_m	F'_v/F'_m	Φ_{PSII}	P700 max (a.u.)
WT	2.97 ± 0.02	3.85 ± 0.06	22.1 ± 0.8	0.47 ± 0.21	63.8 ± 4.7	0.81 ± 0.01	0.60 ± 0.02	0.48 ± 0.02	3251 ± 234
NoM	2.72 ± 0.06*	3.70 ± 0.06*	19.3 ± 1.3*	0.14 ± 0.04*	177.7 ± 16.3*	0.57 ± 0.02*	0.37 ± 0.04*	0.30 ± 0.04*	1587 ± 196*

PSII function was determined on plants either dark-adapted (F_o/Chl, F_v/F_m) or upon illumination at 150 µmol photons m^{-2} s^{-1} for 25 min in the presence of saturating CO_2 (F'_v/F'_m, Φ_{PSII}), the maximum amount of photo-oxidizable PSI RC (P700 max) on dark-adapted leaves. Symbols and error bars show means ± s.d. ($n > 5$). Values that are significantly different (Student's *t*-test, $P < 0.05$) from the wild type (WT) are marked with an asterisk (*). Car, carotenoids; a.u., arbitrary units.

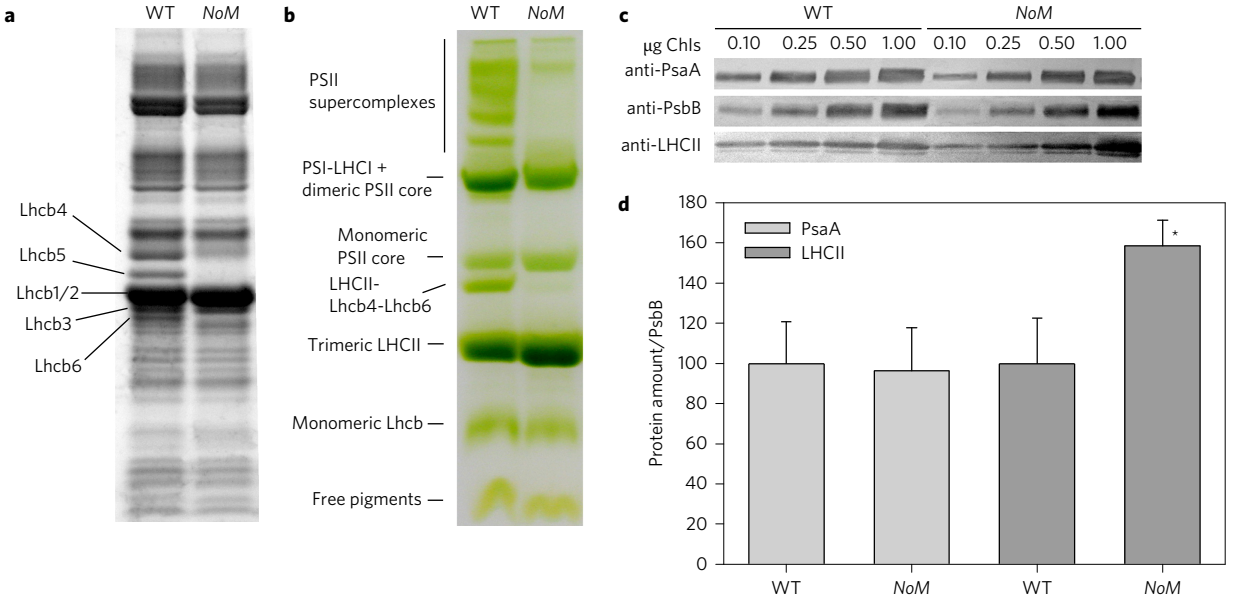

Figure 2 | Biochemical characterization of the *NoM* mutant. a, SDS-PAGE analysis of wild-type (WT) and *NoM* mutant thylakoid proteins performed with the Tris-Tricine buffer system. Selected apoprotein bands are marked. **b**, Thylakoid pigment-protein complexes were separated by non-denaturing Deriphat-PAGE upon solubilization with α-DM (dodecyl-D-maltopyranoside). **c**, Immunoblotting used for the quantification of photosynthetic subunits in the wild-type and mutant thylakoids. Immunoblot analysis was performed with antibodies directed against individual gene products: LHCII subunit, the PSII core subunit PsbB (CP47) and the PSI core subunit (PsaA). Thylakoids corresponding to 0.1, 0.25, 0.5 and 1.0 µg of Chls were loaded for each sample. All samples were loaded on the same SDS-PAGE slab gel. **d**, Results of the immunotitration of thylakoid proteins. Data of PSII antenna subunits were normalized to the core amount, PsbB content and expressed as a percentage of the corresponding wild-type content. Data are expressed as mean ± s.d. ($n = 4$). The significantly different value from wild-type membranes (Student's *t*-test, $P < 0.05$) is marked with an asterisk (*).

from the light-induced quenching of 9-aminoacridine[33] showed that mutant and wild-type chloroplasts had the same ΔpH over a wide range of light intensities (Supplementary Fig. 2b). Consistently, the kinetic of Zea accumulation was the same in both wild-type and *NoM* leaves, and the same de-epoxidation index was measured over different light intensities (Supplementary Fig. 2c,d). These results are consistent with proton-pumping not being affected in *NoM* versus wild-type chloroplasts. Thus, changes in quenching activity are expected to reflect altered efficiency of quenching reactions only.

The NPQ activity of the two genotypes is shown in Fig. 3a. Upon exposure of wild-type plants to saturating irradiance (1,200 µmol photons m^{-2} s^{-1}, 23 °C), NPQ suddenly reached a value of 1.2 in the first minute, followed by a biphasic rise, faster at 1–4 min and then slower, reaching a maximal value of 2.2 upon 12 min of illumination. NPQ of *NoM* underwent an initial rise, followed by a transient decrease. Quenching resumed only after 5 min illumination, after which quenching rapidly rose to 90% of wild-type value at 12 min illumination. This is consistent with three phases of quenching overlapping in wild type: phase 1 (P1, 0–1 min), phase 2 (P2, 1–4 min) and phase 3 (P3, 4–12 min), although P2 is missing in *NoM*. Recovery in the dark was faster and more complete in *NoM* versus wild type. We did not identify a correlation between NPQ amplitude and preflowering growth stages, since similar kinetics of NPQ were measured at different plant ages within the same genotype (Supplementary Fig. 1b).

The initial fast phase P1 of NPQ induction is transient, depends on the trans-thylakoid ΔpH and PsbS and has been proposed to originate in the PSII core complex[34]. The slower kinetic components, P2 and P3, depend on both lumen acidification, Lut and Zea accumulation[15]. In order to further evaluate the modulation of kinetics by Zea, we measured NPQ during two consecutive cycles of HL, separated by a dark relaxation. Zea was synthesized during the first light treatment and was present at the onset of the second illumination period owing to the slow kinetic of the Zea-Viola back-reaction[6]. The resulting kinetics showed that preloading with Zea resulted in a much faster rise of quenching, reaching near maximal amplitude in both genotypes already in P1 with no further increase in P2 and P3. A transient decline of quenching in P2 followed by recovery in P3 was still evident in the mutant trace (Fig. 3b). The kinetic of dark relaxation was still faster than in wild type and the difference increased during the second dark period. Since the kinetic of Zea accumulation was the same in both wild-type and *NoM* leaves (Supplementary Fig. 2c), the differences in quenching kinetics are likely due to differences in the availability of Zea-binding sites. The results of Fig. 3a,b imply that the lack of monomeric LHCs affects NPQ mainly during illumination of dark-adapted leaves. In order to further assess this point, we

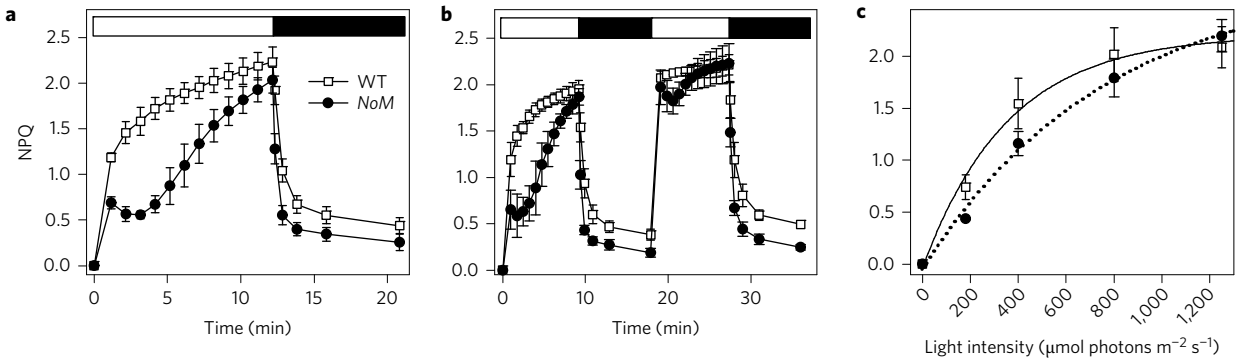

Figure 3 | Kinetics of rise and relaxation of photoprotective energy dissipation. a, Measurements of NPQ kinetics on wild-type (WT) and *NoM* leaves illuminated with 1,200 μmol photons m^{-2} s^{-1}. See Supplementary Fig. 3 for NPQ kinetics of the parental double mutants *koLhb4* and *koLhcb5 Lhcb6*. **b**, NPQ kinetics of wild-type and *NoM* plants during two consecutive periods of illumination with white light (1,200 μmol photons m^{-2} s^{-1}). **c**, Dependence of NPQ amplitude measured at different light intensities. Steady-state photosynthesis was induced by white actinic light; parameters were measured after 25 min of illumination. Symbols and error bars show means ± s.d. ($n > 3$). White and black bars represent light and dark periods.

measured NPQ during steady-state photosynthesis at different light intensities (Fig. 3c), showing that the overall NPQ activity was indeed significantly lower in *NoM* versus wild type at light intensities below 1,000 μmol photons m^{-2} s^{-1}.

In order to verify *in vivo* the differential role of Zea and of other known factors determining NPQ activity, further genetic analysis was undertaken. To this aim, *Arabidopsis NoM* mutants devoid of Zea (*NoM npq1*), Lut (*NoM lut2*) or both (*NoM npq1 lut2*), or lacking the PsbS subunit (*NoM npq4*) were generated. P1 was maintained in the *npq1* and *lut2* mutants, whereas P2 was reduced in *lut2* and both P2 and P3 were reduced in *npq1* with respect to wild type. Contrary to *lut2*, the NPQ kinetic of *NoM lut2* was identical to *NoM* in all components whereas *NoM npq1* retained the P1 component only.

Introducing the *npq1* mutation in wild type and *NoM* had a strong decreasing effect in the NPQ activity of both genotypes (Fig. 4a,b), suggesting Zea-binding to antenna subunits active in NPQ occurred in both genotypes. The effect of introducing the *lut2* mutation was, instead, significant in wild type only (Fig. 4a,b), implying Lut-binding sites active in NPQ were missing in *NoM*. The effect of introducing the double mutation *npq1 lut2* or the *npq4* mutation caused a full depletion of activity in wild-type and *NoM* background (Fig. 4a,b).

The pigment composition of xanthophyll- or PsbS-deficient mutants, in either dark-adapted state or upon 12 min illumination with HL, is shown in Supplementary Table 1. Xanthophyll content was higher in *NoM* mutants with respect to the corresponding genotypes accumulating monomeric LHCs, and β-carotene was the same. Lut was absent in all the *lut2* genotypes, and compensated for by increased Vio. Treatment with HL induced Zea synthesis in *npq4* and *NoM npq4* plants to the same level as in wild type, whereas *lut2* and *NoM lut2* accumulated 2.5-fold more Zea. In *npq1* and *NoM npq1* genotypes, HL did not induce Vio de-epoxidation as in *npq1 lut2* or *NoM npq1 lut2* genotypes. The double illumination experiment (Fig. 4c,d) confirmed that NPQ in the *NoM* mutants was fully dependent on Zea although independent from Lut. This was strikingly different from wild type which depended both on Lut and Zea, in agreement with previous reports[15,35]. In *NoM lut2*, the second actinic illumination was accompanied by an increase in the amplitude of slowly relaxing quenching (qI), the latter being an indicator of photodamage or sustained down-regulation of PSII[4]. The inability of *NoM npq1* plants to undergo qE was maintained even in the second illumination, whereas the increase in max NPQ was mostly due to the higher amplitude of the qI component (Fig. 4d).

From the above results, we conclude that NPQ activity in wild type has three phases: namely, a very fast P1 at the dark-light transition; a second, P2, partially overlapping with P1 due to monomeric LHC proteins, which is absent in *NoM*; and a more slowly activated P3 involving LHCII, retained in *NoM*. The P2 depends on both Lut and Zea, whereas the P3 depends on Zea only. All three components were dependent on PsbS.

Investigations on the mechanism(s) of NPQ. The mechanistic models proposed for excess energy dissipation include (1) the establishment of LHCII aggregates *in vivo*, opening a channel for energy transfer from Chls to the Lut S1 state[19], and (2) the Chl *a* – Zea CT[24], which was proposed to occur within monomeric LHCs[25].

According to the former proposal, the transition into the dissipative state engages a clustering of LHCII proteins into aggregates with low fluorescence yield that can be reproduced *in vitro* by inducing aggregation of purified LHCII antenna proteins in low detergent and low pH[36]. This can be observed *in vivo* by 77 K fluorescence emission spectroscopy of leaves as a decrease of the red emission peak concomitant to an increased far-red emission at 727 nm[37]. In order to determine whether the phases of NPQ described above could be attributed to any of the previously proposed mechanisms, we carried out specific assays: first, we performed 77 K Chl fluorescence quenching experiments on wild-type and *NoM* leaves, either HL-treated using 1,200 μmol photons m^{-2} s^{-1} light, or after recovery of HL-treated leaves in darkness for 10 min[37]. In both wild type and *NoM*, 77 K emission spectra recorded upon HL treatment showed a lower amplitude of the PSII emissions (685 and 695 nm components) with respect to the dark-recovered sample. Instead, the amplitude of the long wavelength component (727 nm) was significantly enhanced (Supplementary Fig. 4). Light minus dark difference spectra clearly showed the HL-induced increase in the 727 nm emission was absent in *npq4* genotypes whereas it was stronger in the case of *NoM* leaves, suggesting the rate of the process undergoing this red-shifted PSII emission, namely the clustering/aggregation of trimeric LHCII[38], was associated with the build-up of NPQ and enhanced in *NoM* with respect to wild type (Fig. 5).

We then proceeded to investigate the relevance of the second quenching mechanism, namely the formation of a CT state between Chl *a* and Zea, which was first observed by ultra-fast pump-probe experiments on isolated thylakoid membranes[24]. In order to verify whether *NoM* was competent in the formation of a Zea^+ radical cation, we measured ultrafast transient absorption (TA) kinetics in isolated thylakoids, before and after inducing qE. The samples were excited at 665 nm and individual TA kinetic traces were measured on spinach, *Arabidopsis* wild-type and *NoM* thylakoids at 1,030 nm, where carotenoid radical cations have substantial absorption[24] (Fig. 6 and Supplementary Fig. 5). In both

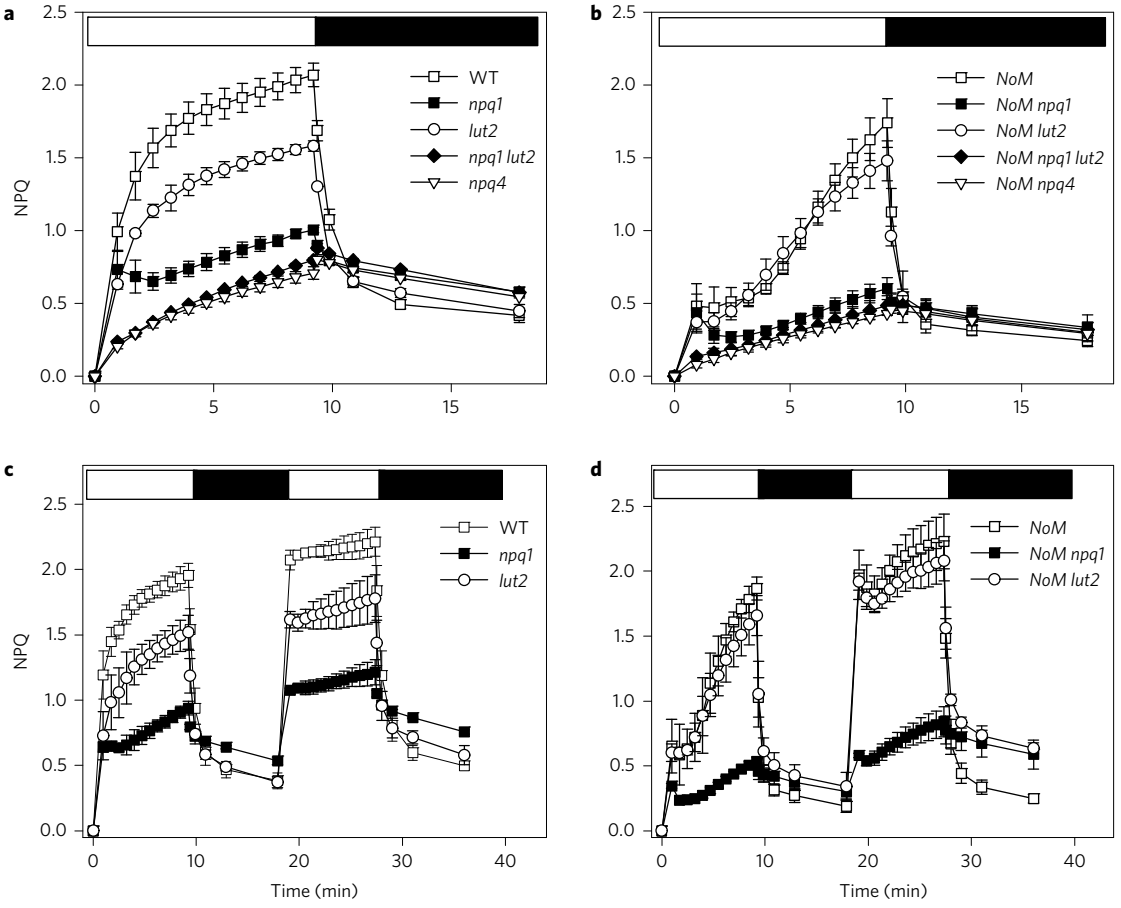

Figure 4 | Kinetics of the formation and relaxation of photoprotective energy dissipation. a,**b**, Measurements of NPQ kinetics on plants either retaining (**a**), or devoid of (**b**), monomeric antennae, and unable to synthesize zeaxanthin (*npq1*), lutein (*lut2*) or PsbS (*npq4*). WT, wild type. **c**,**d**, NPQ kinetics measured on selected genotypes during two consecutive periods of illumination with white light. Leaves were illuminated with 1,200 µmol photons m^{-2} s^{-1}. Symbols and error bars show means ± s.d. ($n > 3$). White and black bars represent light and dark periods.

spinach (Supplementary Fig. 5) and *Arabidopsis* wild-type thylakoids (Fig. 6, upper panel), the differential optical density (ΔOD) traces under actinic light (red lines) revealed additional rise and decay components versus the traces recorded in the absence of qE (black line), thus showing the characteristic pattern of a Zea^+ radical cation signal[24]. The amplitude of the signal was slightly higher in spinach chloroplasts owing to their higher NPQ activity. Thylakoids from *NoM* instead, despite showing NPQ activity, although slightly lower than in wild type, displayed the same kinetics at 1,030 nm (Fig. 6, lower panel) within the experimental error. We conclude that near infrared absorption changes, detected in wild-type thylakoids and reflecting a CT event, can be correlated with the NPQ component associated with monomeric LHCs only. Instead, no TA signals that can be associated with CT could be detected in genotypes retaining LHCII as the only antenna, despite the fact that the LHCII content was increased by 60% in the *NoM* versus wild-type thylakoids.

Discussion

All oxygenic photoautotrophs have mechanisms for regulating the efficiency by which the excited states from absorbed light are transferred to RC for photochemical reactions. Eukaryotic algae and land plants evolved feedback-regulated systems in which thylakoid luminal pH signals excess irradiation. Transduction of the low luminal pH into activation of NPQ reactions requires PsbS in land plants[39]. Pigment interactions, either Chl/Chl pairs[21,22] or Chls/carotenoid pairs[19,23,26], have been proposed to be essential elements of quenching reactions for Chl excited states, thus implying that quenching mechanisms, elicited by the pigment-less subunit PsbS, must occur in interacting pigment-binding subunits of the PSII antenna system. Instead, the organization of PSII–LHCII supercomplexes does not appear to be relevant for NPQ activity since PSII RC level can be reduced by pharmacological treatments or low temperature[17,40], leading to the formation of LHCII-only membranes with enhanced NPQ[17]. The difficulty with identification of quenching sites among LHC gene products is redundancy, since members of the PSII antenna system in *Arabidopsis* are encoded by 14 homologous genes. Reverse genetics has contributed to featuring properties of gene products involved, by showing that quenching reactions are prevented by lack of both Lut and Zea[15] or their ligand LHC proteins[41]. In Lhcb subgroups, down-regulation of Lhcb1[42] and monomeric LHCs[29,30], but not of Lhcb2[43] or Lhcb3[44], affected quenching, thus inciting a lively debate on the mechanisms and localization of quenching reactions in either the monomeric or the trimeric antenna proteins.

Results obtained in the present study from the functional characterization of the *NoM* mutant and by further introducing mutations in this background suggest a series of conclusions.

LHC monomers modulate the middle P2 phase of energy dissipation, namely in the first minutes of transition from darkness to strong illumination (Fig. 3a,b). Slower onset of quenching was previously reported in single KO genotypes[29,30], although the effect was weaker. This evidence indicates that monomeric LHCs collectively contribute to the early phase of the quenching response.

LHCII trimers also participate in quenching but their response rate is slower. Indeed, illumination in the *NoM* genotype leads to

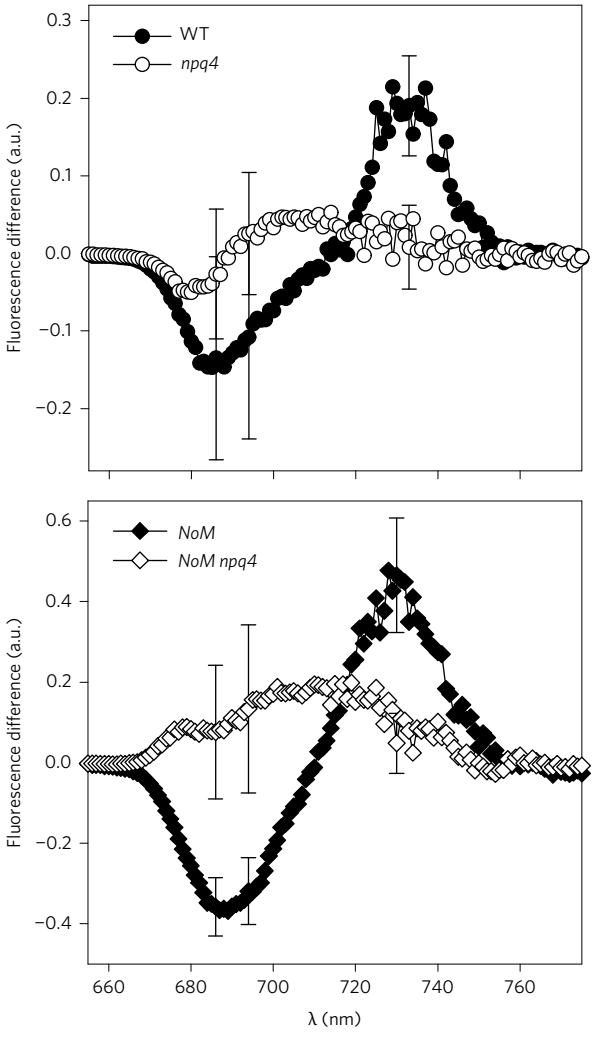

Figure 5 | Spectral changes associated with the formation of NPQ in wild-type, *npq4* and *NoM* genotypes. The 77 K fluorescence emission spectra were recorded from *Arabidopsis* wild-type (WT), *npq4*, *NoM* and *NoM npq4* leaves, either illuminated for 12 min with white actinic light (1,200 μmol photons m^{-2} s^{-1}, RT) or kept for 10 min in darkness upon illumination, to promote NPQ relaxation. Figure displays comparison of light-minus-redark fluorescence difference spectra for *Arabidopsis* wild type versus *npq4* (upper panel) and *NoM* versus *NoM npq4* (lower panel) plants. Error bars represent the s.d. values at 686, 694 and 727 nm, corresponding to eight leaves measured individually for each genotype (for details see ref. 37 and Supplementary Fig. 4).

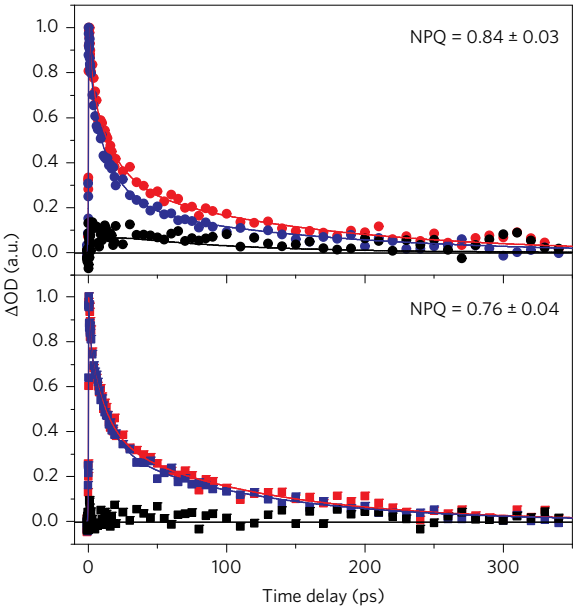

Figure 6 | TA spectroscopy on wild-type and *NoM* thylakoids. TA kinetics have been probed at 1,030 nm on thylakoids of *Arabidopsis* wild type (WT, higher panel) or *NoM* (lower panel) with qE (red line) or without qE (blue line). Difference kinetic traces are reported in black. Symbols show experimental data and solid lines multi-exponential fits.

the same quenching amplitude as wild type only after ~10 min of light. This implies that trimeric and monomeric LHCs synergistically contribute to energy dissipation under the fast-changing conditions caused by variable shading under canopies. When considering the relative abundance of trimeric LHCII versus monomeric complexes in wild type[13] and the further 60% increase in trimeric LHCII observed in *NoM* (Fig. 2d), the specific quenching activity of monomeric LHCs appears far higher than that of trimeric LHCII. The lack of monomeric LHCs leads to dissociation of PSII supercomplexes, confirming that LHCII trimers could be the site of the quenching irrespective of their involvement in PSII supercomplexes[17].

The nature of the quenching reactions is different in monomers versus trimers: the faster-activated P2 in monomers requires both Lut and Zea, whereas the slower-activated P3 in LHCII is dependent on Zea only (Fig. 4b,d), as shown by the phenotype of the *NoM npq1* mutant, hardly distinguishable from the null activity of *NoM npq4* and *NoM npq1 lut2* (Fig. 4b). This indicates that Lut bound to the LHC monomers is responsible for the changes in NPQ observed in the *NoM* mutant, so that deletion of Lut gave rise to no further changes. This is further supported by the results of TA measurements of carotenoid radical cation in thylakoids of wild type versus *NoM*, showing that appearance of the radical cation is associated with the monomeric LHCs (Fig. 6). These findings are fully consistent with previous data on purified LHC proteins showing generation of carotenoid radical cation in LHC monomers and not in LHCII trimers[25]. Moreover, our results show Vio and Lut can substitute for each other in the same quenching site(s) within LHCII, whereas Vio in monomers functions as an inhibitor for quenching. This notion is consistent with evidence that a higher amount of Lut in monomeric LHCs enhances both carotenoid radical cation formation and amplitude of qE[45].

Although the appearance of carotenoid radical cation in wild-type thylakoids under quenching conditions suggests that this mechanism is responsible for quenching in LHC monomers, it can be asked which kind of quenching reaction occurs in trimeric LHCII, leading to sustained fluorescence quenching *in vivo* (Fig. 4b). Previous work suggested LHCII undergoes quenching by clustering in the thylakoid membrane[14], leading to red-shifted 400 ps emission[38] which enhances the amplitude of the 727-nm peak in 77 K emission spectra[37]. In Fig. 5, wild type and *NoM* show an HL-induced 727 nm emission change ($\Delta F_{727\ nm}$). This is PsbS-dependent since it is greatly reduced in *npq4* and *NoM npq4*. The signal is enhanced in *NoM* leaves, in which LHCII content is 60% higher with respect to wild type, implying the $\Delta F_{727\ nm}$ is related to the abundance of trimeric LHCII. These data are consistent with this type of LHCII-dependent quenching being active in both wild type and *NoM*, being the only one in the latter genotype. However, we show that quenching in *NoM* is fully dependent on Zea (Fig. 4) at variance with previous reports[46,47]. Also, NPQ in *NoM* is not affected by the *lut2* mutation, suggesting the processes underlying quenching by LHCII *in vivo* differ in some respect to those induced by aggregation *in vitro*, where Lut was shown to act as a quencher[19]. Our results are consistent with the proposal[48] that quenching sites

might be formed by the interaction of PsbS with the major LHCII complex, with the involvement of a Zea molecule. However, the molecular details of PsbS-mediated LHCII quenching have yet to be determined in future work. Genetic dissection of the interactions between components contributing to LHCII quenching (Fig. 4) allows for at least two hypotheses. First, (1) PsbS and Zea binding to LHCII induce a conformational change in the latter which opens a channel for energy transfer from Chl to the S1 state of a xanthophyll in site L1[19], where Vio or Lut shows the same efficiency (Fig. 4b). Alternatively, (2) it can be proposed that a Chl-Car heterodimer forms between a Zea molecule and a peripheral Chl of LHCII[49,50], leading to a quenching interaction. Although our results point to monomeric LHCs as modulators of the quenching response, it might be asked whether this is consistent with localization of LHC monomers in-between the PSII core complex and trimeric LHCII. Indeed, topological analysis of changes induced in PSII antenna organization upon activation of NPQ has shown that protonated PsbS causes dissociation of CP24 and the LHCII-M trimer from the C2S2M2 supercomplex, thus making CP29 accessible to possible interactors activated by lumen acidification[14], including PsbS itself. The two moieties of the PSII antenna system produced by the dissociation event are, thus, proposed to become the sites for the fast-activated and slow-activated components of NPQ identified by the *NoM* mutant in the present report.

Illumination of dark-adapted *NoM* leaves with saturating light resulted in the fast development of a quenching during the first minute (P1), which transiently reversed in the following 3–4 min (P2); then, quenching resumed and rose to the same amplitude of wild type (P3). P1 is partially affected by either Zea or Lut depletion, and it disappears completely in plants devoid of PsbS (Fig. 4). The fluorescence dynamic of *NoM* leaves is consistent with generation of transient RC quenching, documented both *in vitro*[51] and *in vivo*[34] within the first 1–2 min of illumination. It was detected in wild-type leaves at subsaturating irradiance, whereas it was rapidly converted into a large, antenna-type quenching process at saturating light[34]. In *NoM* genetic background, the RC quenching becomes evident even upon sustained illumination, due to the slower activation of qE. Clearly, PsbS is involved in generation of RC quenching, possibly through direct association to the PSII core complex[52].

We propose that PsbS, upon protonation, increases its affinity for CP29 (and possibly CP26) leading to the disruption of the C2S2M2 supercomplex into a C2S2 moiety and a CP24-LHCII moiety[14], both of which interact with PsbS, although by different modes (Supplementary Fig. 6). Interaction with CP29/CP26 leads to a conformational change, which is favoured by the high rate of Vio/Zea exchange[53], by the presence of proton-binding sites in these two complexes[54] and by the formation of tight interactions between two Chl *a* ligands and either Zea or Lut bound to site L2[25,26,45]. PsbS also interacts with LHCII as shown by the presence of NPQ in the *NoM* mutant, and this interaction requires Zea, but not Lut, for triggering of the quenching. Whether Zea is located in-between PsbS and its LHCII interactor[48] or binds to the V1 site[49,50] is not clear at present and requires further analysis.

Methods

Plant material and growth conditions. Wild-type plants of *Arabidopsis thaliana* (Col-0) and mutants *koLhcb4.1*, *koLhcb4.2*, *koLhcb5* and *koLhcb6* were obtained as previously described[29,30]. Multiple mutant *koLhcb4.1 koLhcb4.2 koLhcb5* (*NoM*) was isolated as previously described[31]. Multiple mutants *NoM npq1*, *NoM npq4*, *NoM lut2* and *NoM npq1 lut2* were obtained by crossing single mutants and selecting progeny by either immunoblotting or HPLC. Plants were grown in a phytotron for 6 weeks at 150 µmol photons m^{-2} s^{-1}, 23 °C, 70% humidity, 8/16 h of day/night.

Membrane isolation. Chloroplasts and stacked thylakoid membranes were isolated as previously described[55].

Pigment analysis. To measure zeaxanthin accumulation, detached leaves floating on water were exposed to 1,200 µmol photons m^{-2} s^{-1} at room temperature (RT, 22 °C). Pigments were extracted from leaf discs with 85% acetone buffered with Na_2CO_3, separated and quantified by HPLC[56].

Spectroscopy. Absorption measurements were performed at RT using an SLM Aminco DW-2000 spectrophotometer. P700 absorption changes of leaves were sampled by weak monochromatic flashes (10-nm bandwidth, 705 nm) provided by light-emitting diodes (JTS10; Biologic Science Instruments).

Gel electrophoresis and immunoblotting. SDS–PAGE analysis was performed using the Tris-Tricine buffer system[57]. Non-denaturing Deriphat-PAGE was performed as described in[58]. For immunotitration, thylakoid samples were loaded for each sample and electroblotted on nitrocellulose membranes, then proteins were detected with alkaline phosphatase-conjugated antibody.

Analysis of Chl fluorescence. PSII function during photosynthesis was measured through Chl fluorescence on whole leaves at RT with a PAM 101 fluorimeter (Heinz–Walz). Chl fluorescence parameters were calculated according to[32]. Colour video images of F_0 (minimal fluorescence from dark-adapted leaves) were obtained with a FluorCam FC 800-C (PSI, Brno, Czech Republic).

Measurement of ΔpH. The kinetics of ΔpH formation across the thylakoid membrane were measured in chloroplast suspension using the method of 9-aminoacridine fluorescence quenching, as previously described[33].

77K fluorescence measurements. The 77 K Chl fluorescence quenching experiments were done according to[37] with minor modifications. Dark-adapted leaves were either illuminated with 1,200 µmol photons m^{-2} s^{-1} of white light at RT for 12 min, or redarkened for 10 min and then immediately frozen in liquid nitrogen. Fluorescence spectra were recorded using a Jobin-Yvon Fluoromax-3 spectrofluorimeter equipped with an optical fibre.

Near infrared TA spectroscopy. Time-resolved experiments to detect the generation of the Car radical cation were performed in a standard pump-probe setup. A KGW amplified laser system (Pharos, Light Conversion) provided the probe wavelength at 1,030 nm and pumped a lab-built non-colinear optical parametric amplifier. The latter provided pump pulses at 665 nm, which were focused to a 220 µm spot at the sample, whereas the probe spot was kept twice smaller. Measured cross-correlation between pump and probe pulses was ~200 fs. A 20 nJ per pulse excitation energy and 200 kHz repetition rate were used for the spinach experiments, whereas 40 nJ per pulse and 20 kHz were used for the *Arabidopsis* experiments. Double-frequency lock-in detection was used to reject high scattering from the sample. Optical choppers operating at 179 and 399 Hz were placed in the pump and probe beams, and TA signal was measured at the sum and difference frequencies[59]. Thylakoid samples with optical density of 0.6–0.8 at the excitation wavelength were kept in the 1 mm path length fused silica optical cell, which was constantly moved in the raster pattern during the experiments. Freshly prepared and activated samples were never measured for longer than 1 h to prevent accumulation of the inactive thylakoids. Dark-adapted kinetics were measured first, followed by HL-induced measurements. HL conditions were induced with 10 min illumination by the 760 µmol photons m^{-2} s^{-1} of white actinic light. A 770-nm pass filter was placed before the detector and a 315–710 nm bandpass filter was placed after the actinic lamp.

Data availability. Sequence data from this article can be found in the *Arabidopsis* Genome Initiative or GenBank/EMBL databases under accession numbers At5g01530 (Lhcb4.1), At3g08940 (Lhcb4.2), At4g10340 (Lhcb5), At1g15820 (Lhcb6), At1g08550 (violaxanthin de-epoxidase), At1g44575 (PsbS) and At5g57030 (lycopene-ε-cyclase). The knock-out lines mentioned in the article were obtained from the NASC under the stock numbers N376476 (*koLhcb4.1*), N877954 (*koLhcb4.2*), N514869 (*koLhcb5*), N577953 (*koLhcb6*) and N505018 (*lut2*).

Received 15 September 2016; accepted 14 February 2017; published 10 April 2017

References

1. Vass, I. *et al.* Reversible and irreversible intermediates during photoinhibition of photosystem II: stable reduced QA species promote chlorophyll triplet formation. *Proc. Natl Acad. Sci. USA* **89,** 1408–1412 (1992).
2. Niyogi, K. K. & Truong, T. B. Evolution of flexible non-photochemical quenching mechanisms that regulate light harvesting in oxygenic photosynthesis. *Curr. Opin. Plant Biol.* **16,** 307–314 (2013).
3. de Bianchi, S., Ballottari, M., Dall'Osto, L. & Bassi, R. Regulation of plant light harvesting by thermal dissipation of excess energy. *Biochem. Soc. Trans.* **38,** 651–660 (2010).
4. Horton, P., Ruban, A. V. & Walters, R. G. Regulation of light harvesting in green plants. *Annu. Rev. Plant Physiol. Plant Mol. Biol.* **47,** 655–684 (1996).
5. Cazzaniga, S., Dall'Osto, L., Kong, S. G., Wada, M. & Bassi, R. Interaction between avoidance of photon absorption, excess energy dissipation and zeaxanthin synthesis against photoxidative stress in *Arabidopsis*. *Plant J.* **76,** 568–579 (2013).

6. Nilkens, M. *et al.* Identification of a slowly inducible zeaxanthin-dependent component of non-photochemical quenching of chlorophyll fluorescence generated under steady-state conditions in *Arabidopsis*. *Biochim. Biophys. Acta.* **1797,** 466–475 (2010).
7. Li, X. P. *et al.* Regulation of photosynthetic light harvesting involves intrathylakoid lumen pH sensing by the PsbS protein. *J. Biol. Chem.* **279,** 22866–22874 (2004).
8. Dominici, P. *et al.* Biochemical properties of the PsbS subunit of photosystem II either purified from chloroplast or recombinant. *J. Biol. Chem.* **277,** 22750–22758 (2002).
9. Fan, M. *et al.* Crystal structures of the PsbS protein essential for photoprotection in plants. *Nat. Struct. Mol. Biol.* **22,** 729–735 (2015).
10. Suga, M. *et al.* Native structure of photosystem II at 1.95 Å resolution viewed by femtosecond X-ray pulses. *Nature* **517,** 99–103 (2015).
11. Jansson, S. A guide to the *Lhc* genes and their relatives in *Arabidopsis*. *Trends Plant Sci.* **4,** 236–240 (1999).
12. Wei, X. *et al.* Structure of spinach photosystem II-LHCII supercomplex at 3.2 Å resolution. *Nature* **534,** 69–74 (2016).
13. Kouril, R., Wientjes, E., Bultema, J. B., Croce, R. & Boekema, E. J. High-light vs. low-light: effect of light acclimation on photosystem II composition and organization in *Arabidopsis thaliana*. *BBA-Bioenergetics* **1827,** 411–419 (2013).
14. Betterle, N. *et al.* Light-induced dissociation of an antenna hetero-oligomer is needed for non-photochemical quenching induction. *J. Biol. Chem.* **284,** 15255–15266 (2009).
15. Niyogi, K. K. *et al.* Photoprotection in a zeaxanthin- and lutein-deficient double mutant of *Arabidopsis*. *Photosynth. Res.* **67,** 139–145 (2001).
16. Havaux, M., Dall'Osto, L. & Bassi, R. Zeaxanthin has enhanced antioxidant capacity with respect to all other xanthophylls in *Arabidopsis* leaves and functions independent of binding to PSII antennae. *Plant Physiol.* **145,** 1506–1520 (2007).
17. Belgio, E., Johnson, M. P., Juric, S. & Ruban, A. V. Higher plant photosystem II light-harvesting antenna, not the reaction center, determines the excited-state lifetime-both the maximum and the nonphotochemically quenched. *Biophys J.* **102,** 2761–2771 (2012).
18. Ruban, A. V., Walters, R. G. & Horton, P. The molecular mechanism of the control of excitation energy dissipation in chloroplast membranes—inhibition of deltapH- dependent quenching of chlorophyll fluorescence by dicyclohexylcarbodiimide. *FEBS Lett.* **309,** 175–179 (1992).
19. Ruban, A. V. *et al.* Identification of a mechanism of photoprotective energy dissipation in higher plants. *Nature* **450,** 575–578 (2007).
20. Niyogi, K. K., Grossman, A. R. & Björkman, O. *Arabidopsis* mutants define a central role for the xanthophyll cycle in the regulation of photosynthetic energy conversion. *Plant Cell* **10,** 1121–1134 (1998).
21. Muller, M. G. *et al.* Singlet energy dissipation in the photosystem II light-harvesting complex does not involve energy transfer to carotenoids. *ChemPhysChem* **11,** 1289–1296 (2010).
22. Wahadoszamen, M., Berera, R., Ara, A. M., Romero, E. & van Grondelle, R. Identification of two emitting sites in the dissipative state of the major light harvesting antenna. *Phys. Chem. Chem. Phys.* **14,** 759–766 (2012).
23. Bode, S. *et al.* On the regulation of photosynthesis by excitonic interactions between carotenoids and chlorophylls. *Proc. Natl Acad. Sci. USA* **106,** 12311–12316 (2009).
24. Holt, N. E. *et al.* Carotenoid cation formation and the regulation of photosynthetic light harvesting. *Science* **307,** 433–436 (2005).
25. Avenson, T. J. *et al.* Zeaxanthin radical cation formation in minor light-harvesting complexes of higher plant antenna. *J. Biol. Chem.* **283,** 3550–3558 (2008).
26. Ahn, T. K. *et al.* Architecture of a charge-transfer state regulating light harvesting in a plant antenna protein. *Science* **320,** 794–797 (2008).
27. Barros, T., Royant, A., Standfuss, J., Dreuw, A. & Kuhlbrandt, W. Crystal structure of plant light-harvesting complex shows the active, energy-transmitting state. *EMBO J.* **28,** 298–306 (2009).
28. Avenson, T. J. *et al.* Lutein can act as a switchable charge transfer quencher in the CP26 light-harvesting complex. *J. Biol. Chem.* **284,** 2830–2835 (2009).
29. de Bianchi, S., Dall'Osto, L., Tognon, G., Morosinotto, T. & Bassi, R. Minor antenna proteins CP24 and CP26 affect the interactions between photosystem II subunits and the electron transport rate in grana membranes of *Arabidopsis*. *Plant Cell* **20,** 1012–1028 (2008).
30. de Bianchi, S. *et al.* *Arabidopsis* mutants deleted in the light-harvesting protein Lhcb4 have a disrupted photosystem II macrostructure and are defective in photoprotection. *Plant Cell* **23,** 2659–2679 (2011).
31. Dall'Osto, L., Unlu, C., Cazzaniga, S. & van Amerongen, H. Disturbed excitation energy transfer in *Arabidopsis thaliana* mutants lacking minor antenna complexes of photosystem II. *Biochim. Biophys. Acta* **1837,** 1981–1988 (2014).
32. Baker, N. R. Chlorophyll fluorescence: a probe of photosynthesis *in vivo*. *Annu. Rev. Plant Biol.* **59,** 89–113 (2008).
33. Johnson, G. N., Young, A. J. & Horton, P. Activation of non-photochemical quenching in thylakoids and leaves. *Planta* **194,** 550–556 (1994).
34. Finazzi, G. *et al.* A zeaxanthin-independent nonphotochemical quenching mechanism localized in the photosystem II core complex. *Proc. Natl Acad. Sci. USA* **101,** 12375–12380 (2004).
35. Pogson, B. J., Niyogi, K. K., Bjorkman, O. & DellaPenna, D. Altered xanthophyll compositions adversely affect chlorophyll accumulation and nonphotochemical quenching in *Arabidopsis* mutants. *Proc. Natl Acad. Sci. USA* **95,** 13324–13329 (1998).
36. Horton, P. *et al.* Control of the light-harvesting function of chloroplast membranes by aggregation of the LHCII chlorophyll-protein complex. *FEBS Lett.* **292,** 1–4 (1991).
37. Lambrev, P. H., Nilkens, M., Miloslavina, Y., Jahns, P. & Holzwarth, A. R. Kinetic and spectral resolution of multiple nonphotochemical quenching components in *Arabidopsis* leaves. *Plant Physiol.* **152,** 1611–1624 (2010).
38. Holzwarth, A. R., Miloslavina, Y., Nilkens, M. & Jahns, P. Identification of two quenching sites active in the regulation of photosynthetic light-harvesting studied by time-resolved fluorescence. *Chem. Phys. Lett.* **483,** 262–267 (2009).
39. Li, X. P. *et al.* A pigment-binding protein essential for regulation of photosynthetic light harvesting. *Nature* **403,** 391–395 (2000).
40. Caffarri, S., Frigerio, S., Olivieri, E., Righetti, P. G. & Bassi, R. Differential accumulation of *Lhcb* gene products in thylakoid membranes of *Zea mays* plants grown under contrasting light and temperature conditions. *Proteomics* **5,** 758–768 (2005).
41. Briantais, J.-M., Hodges, M. & Moya, I. in *Progress in Photosynthesis Research II* (ed. J. Biggins) 705–708 (Nijhoff Publishers, 1987).
42. Pietrzykowska, M. *et al.* The light-harvesting chlorophyll a/b binding proteins Lhcb1 and Lhcb2 play complementary roles during state transitions in *Arabidopsis*. *Plant Cell* **26,** 3646–3660 (2014).
43. Leoni, C. *et al.* Very rapid phosphorylation kinetics suggest a unique role for Lhcb2 during state transitions in *Arabidopsis*. *Plant J.* **76,** 236–246 (2013).
44. Damkjaer, J. *et al.* The photosystem II light-harvesting protein Lhcb3 affects the macrostructure of photosystem II and the rate of state transitions in *Arabidopsis*. *Plant Cell* **21,** 3245–3256 (2009).
45. Li, Z. *et al.* Lutein accumulation in the absence of zeaxanthin restores nonphotochemical quenching in the *Arabidopsis thaliana npq1* mutant. *Plant Cell* **21,** 1798–1812 (2009).
46. Lambrev, P. H. *et al.* Functional domain size in aggregates of light-harvesting complex II and thylakoid membranes. *BBA-Bioenergetics* **1807,** 1022–1031 (2011).
47. Miloslavina, Y. *et al.* Far-red fluorescence: a direct spectroscopic marker for LHCII oligomer formation in non-photochemical quenching. *FEBS Lett.* **582,** 3625–3631 (2008).
48. Wilk, L., Grunwald, M., Liao, P. N., Walla, P. J. & Kuhlbrandt, W. Direct interaction of the major light-harvesting complex II and PsbS in nonphotochemical quenching. *Proc. Natl Acad. Sci. USA* **110,** 5452–5456 (2013).
49. Liu, Z. *et al.* Crystal structure of spinach major light-harvesting complex at 2.72 Å resolution. *Nature* **428,** 287–292 (2004).
50. Caffarri, S., Croce, R., Breton, J. & Bassi, R. The major antenna complex of photosystem II has a xanthophyll binding site not involved in light harvesting. *J. Biol. Chem.* **276,** 35924–35933 (2001).
51. Weis, E. & Berry, J. A. Quantum efficiency of photosystem II in relation to energy dependent quenching of chlorophyll fluorescence. *Biochim. Biophys. Acta* **894,** 198–208 (1987).
52. Haniewicz, P. *et al.* Isolation of monomeric photosystem II that retains the subunit PsbS. *Photosynth. Res.* **118,** 199–207 (2013).
53. Morosinotto, T., Baronio, R. & Bassi, R. Dynamics of chromophore binding to Lhc proteins *in vivo* and *in vitro* during operation of the xanthophyll cycle. *J. Biol. Chem.* **277,** 36913–36920 (2002).
54. Walters, R. G., Ruban, A. V. & Horton, P. Identification of proton-active residues in a higher plant light-harvesting complex. *Proc. Natl Acad. Sci. USA* **93,** 14204–14209 (1996).
55. Casazza, A. P., Tarantino, D. & Soave, C. Preparation and functional characterization of thylakoids from *Arabidopsis thaliana*. *Photosynth. Res.* **68,** 175–180 (2001).
56. Gilmore, A. M. & Yamamoto, H. Y. Zeaxanthin formation and energy-dependent fluorescence quenching in pea chloroplasts under artificially mediated linear and cyclic electron transport. *Plant Physiol.* **96,** 635–643 (1991).
57. Schägger, H. & von Jagow, G. Tricine-sodium dodecyl sulfate-polyacrylamide gel electrophoresis for the separation of proteins in the range from 1 to 100 kDa. *Anal. Biochem.* **166,** 368–379 (1987).
58. Havaux, M., Dall'Osto, L., Cuine, S., Giuliano, G. & Bassi, R. The effect of zeaxanthin as the only xanthophyll on the structure and function of the photosynthetic apparatus in *Arabidopsis thaliana*. *J. Biol. Chem.* **279,** 13878–13888 (2004).
59. Augulis, R. & Zigmantas, D. Two-dimensional electronic spectroscopy with double modulation lock-in detection: enhancement of sensitivity and noise resistance. *Opt. Express.* **19,** 13126–13133 (2011).

Acknowledgements

This work was supported by the EEC projects ACCLIPHOT (PITN-GA-2012-316427) and SE2B (675006–SE2B) to R.B. Work in Lund was supported by LaserLab Europe, the Swedish Research Council and the Knut and Alice Wallenberg Foundation. The work of K.K.N. and G.R.F. was supported by the Director, Office of Science, Office of Basic Energy Sciences, of the US Department of Energy under Contract No. DEAC02-05CH11231 and the Chemical Sciences, Geosciences and Biosciences Division, Office of Basic Energy Sciences under field work proposal 449B. L.D.'s work was supported by international mobility programme CooperInt 2011/2014, University of Verona.

Author contributions

R.B., K.K.N. and G.R.F. conceived the work and designed the experiments. L.D., S.C. and M.B. performed all the experiments for the isolation of mutants, and their physiological and biochemical characterization. D.Z. coordinated and performed the transient absorption spectroscopy experiments. D.P. and K.Z. contributed to the time resolved analysis experiments. All of the authors contributed to writing the manuscript. All of the authors discussed the results and commented on the manuscript.

Additional information

Supplementary information is available for this paper.

Reprints and permissions information is available at www.nature.com/reprints.

Correspondence and requests for materials should be addressed to R.B.

How to cite this article: Dall'Osto, L. *et al.* Two mechanisms for dissipation of excess light in monomeric and trimeric light-harvesting complexes. *Nat. Plants* **3,** 17033 (2017).

Publisher's note: Springer Nature remains neutral with regard to jurisdictional claims in published maps and institutional affiliations.

Competing interests

The authors declare no competing financial interests.